On the migration of {332} <110> tilt grain boundary in bcc metals and further nucleation of {112} twin

N. Kvashin[1], A. Ostapovets[2], N. Anento[1], A. Serra[1]

[1]Department of Civil & Environmental Engineering, Universitat Politècnica de Catalunya, Campus Nord, C-2, Jordi Girona, 1-3, 08034 Barcelona, Spain

[2]Department of Experimental Studies and Modelling of Structure, Institute of Physics of Materials, Czech Academy of Sciences, Žižkova 22, 61600 Brno, Czech Republic

Abstract

{332} <110> tilt grain boundaries (GB) move conservatively under a shear stress by the creation and glide of disconnections. When crystal dislocations interact with the GB they are absorbed and transformed into GB dislocations (GBD). The behaviour of GBDs under shear stress depends on the orientation of the Burgers vector and sense of shear stress. There are two possible scenarios: a) the GBD moves together with the GB in a compensated climb, then plastic deformation is accommodated by shear-coupled GB migration; b) the GBD is sessile because it cannot undergo a compensated climb when interacting with the disconnections. If so, the sessile GBD is the nucleus of a {112} twin. The nucleation of the twin is produced by the pileup of disconnections at both sides of the GBD. Then, plastic deformation is accommodated by the combination of the motion of the {332} GB and the growth of {112} twins inside the grain.

1. Introduction

Grain boundaries (GB) play an important role in the mechanical response of polycrystalline metals and alloys. The sustainability of the macroscopic deformation is defined by both, the propagation of dislocation-mediated slip through grains, ruled by the interaction of dislocations with the GB [1-3], and the activation of atomic processes that are intrinsic to the GB. Those processes are the creation of GB dislocations that favour the shear-coupled GB migration [4,5], nucleation of dislocations [6, 7] and the nucleation of twins [7,8,9]. This complex scenario of plastic deformation is firstly dependent on the atomic structure of the GB. Thus, a dislocation can be absorbed, transmitted or reflected when interacting with a GB and the interaction may leave some residual products at the GB that can either help or impede the displacement of the GB.

There are two main crystallographic restrictions for these reactions, i.e., the conservation of Burgers vector (BV) and the set of possible interfacial defects. The former, links the BV of the entrant dislocation with the GBDs produced during the interaction; the latter, described by the theory of interfacial defects [10, 11], establishes that the BV of a GBD is the difference of broken symmetries of the crystals that form the

GB (λ=upper and μ= lower, hereafter). An efficient tool for the characterization of all possible BV of GBDs is the dichromatic pattern formed by the superposition of the lattice sites of both crystals, λ and μ, with the plane of the GB in common (fig.1). The sites of the common plane being the origin for the symmetry vectors of each crystal, $\vec{t}_\lambda$ and $\vec{t}_\mu$, any arrow from μ site to λ site is a possible BV of a GB line defect ($\vec{b} = \vec{t}_\lambda - \vec{t}_\mu$). Thus, GBDs are intrinsic line defects of the GB. When they have, in addition, step character they are named disconnections [10-12] and are characterized by (***b***, *h*) where ***b*** is the BV and *h* is the step height. We refer to the Burgers vectors as $\boldsymbol{b}_{n/m}$, the subscripts denoting the heights of the interfacial step associated with the core defects in units of the spacing of (3-32) lattice plane. This means that a disconnection can be represented as the contact of a step with height of n interplanar distances in the λ crystal and m interplanar distances in the μ crystal. We name elementary disconnections (EDisc) those that, by gliding along the GB, accommodate shear by the BV and transform one crystal into the other in the stepped region of the GB, advancing the GB by *h* [12 -15]. The motion of EDisc along the GB couples shear with migration. The BV of the EDisc is parallel to the GB, $\boldsymbol{b}_{n/n,}$ for the disconnection to glide along the GB, and it is generally small.

Shear-coupled GB migration (SCGBM) is an efficient mechanism for the accommodation of plastic deformation [4, 5, 16, 17]. For this to occur it is necessary that EDisc are created at the GB in a continuous way either as dipoles in the pristine GB or be produced by a source of disconnections that should move together with the GB. During the motion of these EDisc along the GB they may encounter obstacles, such as segregated impurities or clusters of point defects, and they interact with other intrinsic defects of the GB, namely other GBDs. While the interaction with impurities and clusters may increase the critical resolved shear stress but does not change its characteristics (***b***, h) [18], the interaction with other GBDs (with or without step) may result in a new sessile GBD. If so, this reaction may effectively inhibit the disconnection mobility or initiate a more complex process, for example, the nucleation of a twin. The latter reactions are linked to the BV of the reacting defects and, consequently, directly related to the atomic structure of the GB. For some GBs, the reaction of the EDisc with a sessile GBD (with or without step) is mediated by a climb-compensated mechanism [19], which allows both, the glide of the EDisc and the motion of the GBD following the GB [20-22]. These constraints would justify that SCGBM is produced in specific GBs and there is a limited number of deformation twins for each crystal structure.

There is extensive computational and experimental evidence of SCGBM in hcp [5] and fcc [4,23-29] metals since it produces the growth of deformation twins [30], which are abundant in these crystal structures. SCGBM has been less reported in bcc metals despite the fact that this mechanism occurs in this crystal structure and it is crucial for the understanding of the growth of {332} twin and, specially, its conjugate {112} twin [21]. The role of triple junctions in the creation of disconnections treated in the continuous gives a significant theoretical frame [31, 32].

The reaction at the GB may depend on whether there is only one crystal dislocation interacting with the GB or a pileup of crystal dislocations. In the interaction of the (332)

GB with a pileup of dislocations, described in [33], there is a sequential absorption of the dislocations that leads to the formation of a new asymmetric GB interface of {112}/{110} type, which grows with the number of dislocations supplied. If the reaction at the GB is produced by only one crystal dislocation, producing a single GBD, the evolution of the GB may be different, as detailed below. The crystallographic analysis of the interaction with a single dislocation supplies a list of possible reactions [34] but an atomic simulation is needed to discern which of them occur and which processes are feasible in the presence of other dislocations. The experimental research on β-Titanium alloys [35, 36] has proved the existence of profuse {332} twinning. The combination of strength and ductility of such alloys has been attributed to the low stress of nucleation and growth of such twins and the blocking action of the twin boundaries in slip deformation. To elucidate the dislocation - {332} interface interaction at the atomic level will help in the progress of its mechanical properties.

In this paper we present, first, the GBD's created by the interaction of the {332} tilt GB with a crystal dislocation. Then, we describe, in terms of the crystallography involved, the stress-mediated atomic level processes at the GB that accommodates plastic deformation. These processes include the creation of EDisc and their interaction with the existing GBD's that lead to the displacement of the GB and, in some cases, to the nucleation of a (112) twin.

2. Methodology

Molecular dynamics simulator LAMMPS [37] has been applied to study the interaction between the $(3\bar{3}2)$ GB and the crystal dislocations. The simulations in this study are performed at a temperature T=0K. The principal axes of the upper crystal (λ) were oriented along $X = [1\bar{1}\bar{3}]_\lambda$; $Y = [110]_\lambda$; $Z = [3\bar{3}2]_\lambda$. The axes for the lower crystal (μ) were rotated anticlockwise by 50.48^0.The simulations performed in [30] have shown that the mechanism of interaction is common to the bcc metals studied (Fe, Cr and W) although the physical properties are material dependent. In order to clarify the atomic level mechanisms occurring at the interaction with a single dislocation, we have chosen the interatomic potential representing bcc-Fe. As in [33], the embedded-atom method (EAM) potential used is the Ackland et al., fitted to reproduce properties of dislocation lines obtained from DFT [38]. The accuracy of the potential in the study of <110> tilt GBs was checked in [39]. Each simulation begins with a static relaxation, i.e. energy minimization and a relaxed bicrystal without residual defects is obtained. Semi-static approach is used, namely, each increment of strain is introduced by applying deformation to the whole box for a fixed time followed by a relaxation.

The MD simulation box consisted of a symmetric bicrystal with an initially coherent symmetric tilt GB interface in the middle. Approximate dimensions of the cell size were 80 × 4 × 40 lattice vectors along the corresponding directions with a total number of atoms ~ 600.000. Periodic boundary conditions were imposed along the [110] tilt axis and $[1\bar{1}\bar{3}]$ axis along the GB, with fixed boundaries in the directions perpendicular to

the interface. The crystal dislocations are introduced along {112} glide planes for edge dislocations and along a {110} plane for the mixed dislocation using Atomsk software [40]. An incremental shear strain is applied in order to move the dislocations to initiate an interaction with the interface. When an elementary disconnection ($\boldsymbol{b}_{2/2}$) cross the periodic boundary conditions, the GB is displaced by *h* along its normal. The stress state of the system is recorded after each increment of strain. The open visualization tool OVITO is used for visualization and analysis of atomistic simulation data [41].

3. Results

3.1 Dichromatic pattern of the $(3\bar{3}2)$ GB and elementary disconnection ($\boldsymbol{b}_{2/2}$)

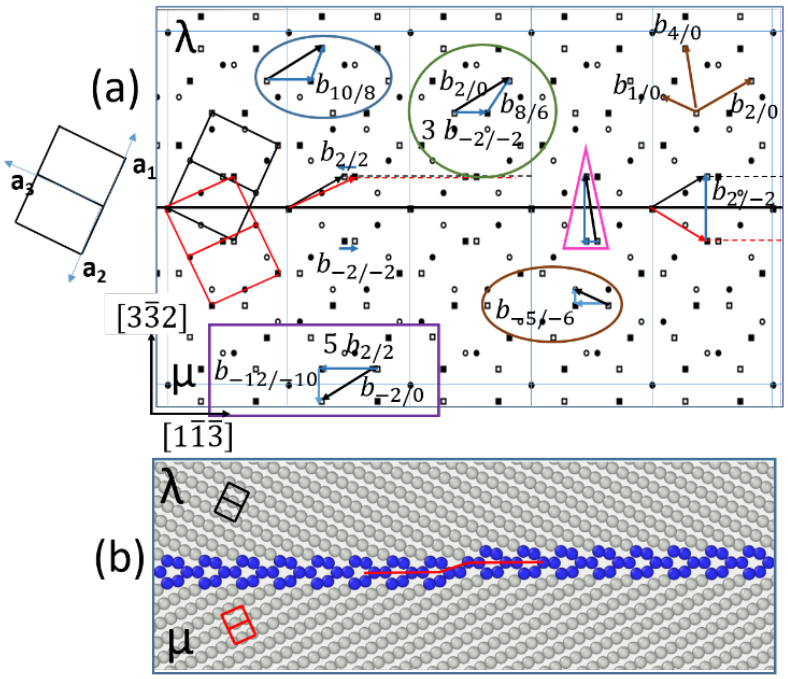

Figure 1. a) [110] projection of the dichromatic pattern (DP) of the $(3\bar{3}2)$ GB showing the Burgers vectors of the EDisc's ($\boldsymbol{b}_{\pm2/\pm2}$), the crystal dislocations ($\boldsymbol{b}_{n/0}$) interacting with the GB and few reactions showing GBD's (see text). The CSL is indicated in pale blue. The unit cell of λ crystal shows the principal axes a_i. b) [110] projection of the $(3\bar{3}2)$ GB with a $\boldsymbol{b}_{2/2}$disconnection stepping up the GB. The unit cells of crystals are represented in black (λ) and red (μ).

Fig.1a shows the dichromatic pattern (DP) of the $(3\bar{3}2)$GB in projection along the tilt axis [110]. The dislocations of the λ (white crystal) that interact with the GB (brown vectors on the top right) are named as $\boldsymbol{b}_{2/0} = \frac{1}{2}[1\bar{1}\bar{1}]$ (edge) $\boldsymbol{b}_{4/0} = \frac{1}{2}[1\bar{1}1]$ (edge) and $\boldsymbol{b}_{1/0} = \frac{1}{2}[111]$(mixed). The EDisc, $\boldsymbol{b}_{2/2}$,is the difference between the translation vector of the λ crystal (black arrow) and the μ crystal (red arrow) as: $\boldsymbol{b}_{2/2} = \frac{1}{2}[1\bar{1}\bar{1}]_\lambda - [00\bar{1}]_\mu = \frac{1}{22}[\bar{1}13]_\lambda$[33]. The dotted lines indicate the position of the GB on the right of the core of the disconnection showing that it steps up the GB by two $(3\bar{3}2)$ planes. Thus, when

the disconnection glides to the left it transforms λ crystal to μ crystal and the GB moves two planes upwards. Notice that the shear imposed by the BV of the disconnection moves black squares into white squares but the sites below represented by circles must do an extra displacement (shuffle) to restore the perfect μ lattice [15]. Fig.1b shows the relaxed $(3\bar{3}2)$ GB containing a $\boldsymbol{b}_{2/2}$ disconnection (the red line is a guide for the eye).

In the following, we describe, in section 3.2, the transformation of crystal dislocations at the GB that are represented in the DP as sum of vectors within a circle, ellipsoid, rectangle and triangle respectively. For each GBD obtained, the response of the faceted GB to an external shear stress is described in section 3.3.

3.2 Interaction of the ½ <111> dislocation with the $(3\bar{3}2)$ GB

The crystal dislocations with BV ½ <111> are fully absorbed by the GB. The reaction and final defects at the GB depend on the orientation of the glide plane, the sign of the BV and the edge or mixed character of the dislocation, considering that in the simulations the dislocation line is always along the [110] tilt axis of the GB. The interaction follows the conservation of BV and, in all interactions, the dislocation transforms into a disconnection with a riser, faceting the GB, and several EDisc that glide away $\left(\vec{b}_{Xtal} = \vec{b}_{GBD} + n\,\vec{b}_{EDisc}\right)$. For a given interaction, the number of EDisc depends upon the temperature, as reported in the study of the interaction of the GB with a pileup of dislocations [33].

3.2.1 Edge dislocation with Burgers vector inclined 29.5°

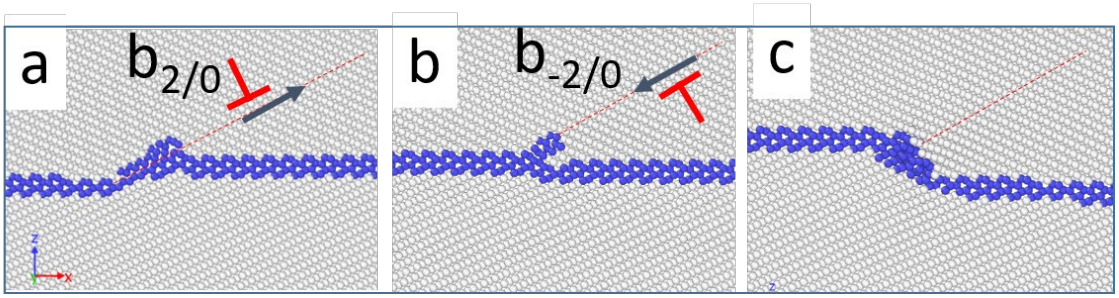

Figure 2. Interaction of the $(3\bar{3}2)$ GB with an edge dislocation (red symbol). a) Dislocation BV forming an acute angle ($b_{2/0}$): The riser of the disconnection *is along the glide plane b) & c) Dislocation BV forming an obtuse angle ($b_{-2/0}$); there is an initial repulsion; the dislocation is absorbed if enough stress is applied: (b) before absorption and (c) after absorption; the riser of the* disconnection *is inclined to the glide plane shown as a dashed red line.*

Fig.2 shows the GB after the interaction with edge dislocations inclined 29.5°. Comparing fig.2a and figs. 2b&c we can observe that the reaction depends on the sign of the entrant dislocation.

Interaction with $b_{2/0}$: When the BV forms an acute angle with the GB (fig.2a) and the dislocation is at a distance of about three lattice parameters, the GB attracts the dislocation and absorbs it. The dislocation transforms into a disconnection, as shown in fig.2a, and several EDisc that glide away. The riser of the disconnection is along the glide plane of the dislocation forming a facet $\{112\}_{\lambda}/\{110\}_{\mu}$.

The BV of the disconnection depends on the number of EDisc emitted, which may be three or four depending on the temperature and the local stress. The reactions are:

$$b_{2/0} = \frac{1}{2}[1\bar{1}\bar{1}] = \frac{1}{11}[4\bar{4}\bar{1}] + 3\frac{1}{22}[1\bar{1}\bar{3}] = b_{8/6} + 3b_{-2/-2} \quad (1)$$

$$b_{2/0} = \frac{1}{2}[1\bar{1}\bar{1}] = \frac{1}{22}[7\bar{7}1] + 4\frac{1}{22}[1\bar{1}\bar{3}] = b_{10/8} + 4b_{-2/-2} \quad (2)$$

The reaction (1) occurs in a static simulation (T=0K) with relaxation after each strain increment. The reaction (2) occurs in a dynamic simulation at T=300K reported in [33]. The dependence on the local stress is evidenced when the incident dislocation is the first of a pileup of dislocations, as shown in [33].

The reactions (1) and (2) are represented in the DP of fig.1a. In the green circle the BV of the crystal dislocation $b_{2/0}$ (black) is decomposed into the BV of the disconnection, $b_{8/6}$, and three $b_{-2/-2}$ EDisc (blue). The riser of the disconnection (fig.2a) intersect eight $(3\bar{3}2)$ planes of the λ crystal and six planes of the μ crystal. The reaction (2) is represented inside the blue ellipsoid at the top-left of the DP. The location in the DP of the BVs of the GBDs indicates the step high of the riser. These two disconnections have the same behaviour under deformation. In fact, one transforms into the other by emitting/adding a $b_{-2/-2}$ disconnection.

Interaction with $b_{-2/0}$: When the BV forms an obtuse angle with the GB (fig.2b), there is an initial repulsion between the dislocation and the GB. If an external stress is applied, the dislocation overcomes the repulsion and it is linked to the GB but it does not change its BV. When the shear stress is about 1.3GPa, there is absorption of the dislocation. The reaction produces a disconnection and several EDisc but there is a main difference with $b_{2/0}$: the riser of the disconnection forms an angle of 126 degrees to the glide plane of the dislocation forming a facet $\{110\}_\lambda/\{112\}_\mu$ (see fig.2c). The number of EDisc is temperature dependent and varies from five ($\leq$ 150K) to seven (at 900K) as reported in [33]. The reaction between $b_{-2/0}$ and the GB is marked in the DP of fig.1a with a purple rectangle:

$$b_{-2/0} = \frac{1}{2}[\bar{1}11] = \frac{1}{11}[\bar{3}32] + 5\frac{1}{22}[\bar{1}13] = b_{-12/-10} + 5b_{2/2} \quad (3)$$

The BVs of the GBDs are calculated by Volterra operations, as the difference of two translation vectors from the upper and lower crystals respectively obtained from a Burgers circuit (see [42], for example). The BV is double-checked by calculating the BV as the difference of the initial crystal dislocation and the produced EDiscs.

If a pileup of crystal dislocations would follow the first one, in the two reactions studied with $b_{2/0}$ and $b_{-2/0}$, the reactions would be the same as for the single dislocation and the second dislocation would increase the length of the riser created by the first one [33].

3.2.2 Edge dislocation with Burgers vector inclined 100°

There is attraction and absorption by the GB of the $b_{4/0}$ dislocation. The reaction is presented in the DP of fig.1a inside a pink triangle:

$$b_{4/0} = \frac{1}{2}[1\bar{1}1] = \frac{2}{11}[3\bar{3}2] + \frac{1}{22}[\bar{1}13] = b_{2/-2} + b_{2/2} \quad (4)$$

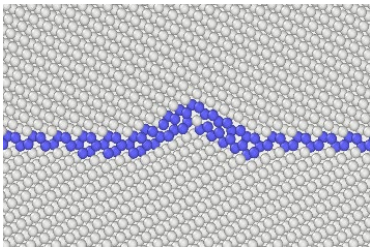

Figure 3. Core of the $b_{2/-2}$ GBD split into $b_{12/10}$ + $b_{-10/-12}$

The BV of the GBD is presented on the right of the DP as the difference of two translation vectors $t_\lambda = \frac{1}{2}[1\bar{1}\bar{1}]_\lambda$ (black) and $t_\mu = \frac{1}{2}[1\bar{1}\bar{1}]_\mu$ (red). The GBD could be imagined as cutting the λ crystal along the black dotted line and the μ crystal along the red dotted line. After joining the two crystals the generated GBDdoes not step the GB.

Under relaxation, the core of the $b_{2/-2}$ GBD is decomposed into two GBD's, each of them with a facet, as shown in fig 3.

The reaction is as follows:

$$b_{2/-2} = b_{12/10} + b_{-10/-12} = \frac{1}{11}[3\bar{3}2] + \frac{1}{11}[3\bar{3}2] = \frac{2}{11}[3\bar{3}2]. \quad (5)$$

If $b_{4/0}$ is the leader of a dislocation pileup gliding towards the GB [33], there is absorption and creation of the $b_{2/-2}$ but there is no relaxation into the facetted core due to the stress field of the next dislocation of the pileup. In fact, the GB is a strong barrier for the glide of this dislocation pileup because even under a stress of 9.5 GPa parallel to the dislocation glide plane the second dislocation cannot be either absorbed by the GB or react with the $b_{2/-2}$ GBD [33].

The crystal dislocation with opposite BV, i.e. $b_{-4/0} = \frac{1}{2}[\bar{1}1\bar{1}]$, does not transform into the $b_{2/-2}$ GBD. Indeed, there is repulsion of the $b_{-4/0}$ dislocation by the GB. The dislocation overcomes the repulsion if a shear stress of 1.3GPa is applied. Then, the dislocation stays attached to the GB but it keeps its BV. The same behavior is found when a pileup of dislocations follows the first one.

3.2.3 Mixed dislocation

The mixed dislocation $\boldsymbol{b}_{1/0} = \frac{1}{2}[111]$ gliding along the $(1\bar{1}0)$ plane interacts with the GB under a shear stress of about 500MPa. Since the screw part ($\frac{1}{2}[110]_\lambda$) is along the tilt axis, it is common to both, the crystal dislocation and the GBD created by the interaction. The reaction produced emits three EDisc $\boldsymbol{b}_{2/2}$ that run away and a disconnection with a riser along the glide plane of the dislocation forming a facet $(1\bar{1}0)_\lambda/(1\bar{1}2)_\mu$. The reaction is plotted in the DP of fig.1a inside a brown ellipsoid below the interface.

$$\boldsymbol{b}_{1/0} = \frac{1}{2}[001] + \frac{1}{2}[110] = \frac{1}{22}[3\bar{3}2] + \frac{1}{2}[110] + \frac{3}{22}[\bar{1}13] = \boldsymbol{b}_{-5/-6} + 3\boldsymbol{b}_{2/2} \quad (6)$$

The reaction with the dislocation of opposite sign $\boldsymbol{b}_{-1/0}$ occurs at about 600MPa and the disconnection produced has a riser inclined to the glide plane with a facet $(1\bar{1}2)_\lambda/(1\bar{1}0)_\mu$.

$$\boldsymbol{b}_{-1/0} = \frac{1}{2}[00\bar{1}] + \frac{1}{2}[\bar{1}\bar{1}0] = \frac{1}{22}[\bar{2}2\bar{5}] + \frac{1}{2}[\bar{1}\bar{1}0] + \frac{2}{22}[1\bar{1}\bar{3}] = \boldsymbol{b}_{3/4} + 2\boldsymbol{b}_{-2/-2} \quad (7)$$

Notice that the orientation of risers relative to the glide plane (see fig.9 in section 3.3.4) is comparable to the ones of the disconnections produced by the dislocations $\boldsymbol{b}_{2/0}$and $\boldsymbol{b}_{-2/0}$.The orientation of the risers determines the stress necessary for the accommodation of a pileup of dislocations approaching from the same glide plane [33].

3.3 Displacement of a $(3\bar{3}2)$ GB under an applied shear stress

In the pristine $(3\bar{3}2)$ GB, dipole pairs of disconnections are created when the shear stress is $\sigma_{xz} = 1.45$ GPa (at T= 0K). Disconnections of opposite signs run in opposite directions under the shear stress and displace the GB by two planes per dipole, as shown in fig. 4a. The resolved shear stresses to move the $\boldsymbol{b}_{\pm 2/\pm 2}$ EDiscs to the right is $|\sigma_{xz}|$ =550 MPa, whereas to move them to the left is$|\sigma_{xz}| = 620$ MPa.

When the shear stress is positive (fig.4a,b), the GB is displaced upwards (transforms λ crystal into μ crystal); the process is reversible and the GB is displaced downwards when the shear stress is negative as shown schematically in fig. 4c,d.The asymmetry of stresses favours the glide of EDisc that are moving to the right. This asymmetry may influence the displacement of the GB at low temperatures, especially if other GB defects are present.

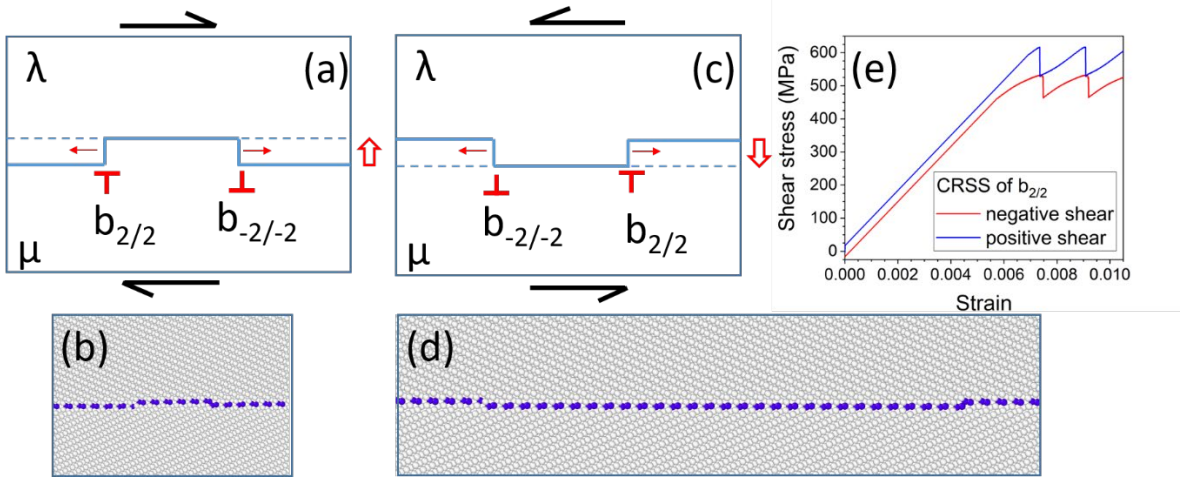

Figure 4. Dipole of disconnections gliding under an applied shear stress; the GB is displaced upwards (a,b) and downwards (c.d), as indicated by big red arrows.(e) Critical resolved shear stress (CRSS) of the $\boldsymbol{b}_{2/2}$ *disconnection under a positive and negative shear stresses.*

If a stress concentrator exists in the GB, the stress necessary to create the dipole of disconnections is smaller [21]. For instance, a GBD may act as a source of EDisc. If the GBD can follow the GB during its displacement, then the source is effective and a sustained SCGBM occurs. This is found in the {112}<110> tilt GB [21] but in the {332}<110> tilt GB, not all GBD can follow the GB; an example of sustained motion of the GBD is shown in fig. 5. As described in section 3.2, there is a variety of GBDs at the {332} GB depending on the characteristics of the crystal dislocation interacting with the GB. The interaction of a GBD with the glissile EDiscs, when a shear stress is applied, depends on the GBD and the sense of the shear stress.

In the following, we describe the effect of an external shear stress on the displacement of the GB as a function of the GBD. Initially, the GBD is created by a reaction with the

crystal dislocation. Then, a shear stress is applied to the system containing the GB with the stable GBD. To study the displacements upwards and downwards of the GB, two senses of the shear stress are applied for each GBD.

3.3.1 GB with a disconnection produced by the interaction with $\boldsymbol{b}_{2/0}$ dislocation(29.5°)

The crystal dislocation $\boldsymbol{b}_{2/0}$, attracted by the GB, originates a disconnection (either $b_{8/6}$ or $b_{10/8}$ as described above). When a shear stress is applied, the disconnection acts as a source of pairs of $\boldsymbol{b}_{2/2}$ EDisc of opposite sign that glide along the GB allowing its displacement, as shown in fig. 5. The mechanism, originally described in [19, 20, 22] for the {10-12} twin hcp metals, occurs in bcc metals for certain tilt GBs such as the {112} twin [16, 21] and its conjugate the {332} twin as described in [33]. The scheme in fig.5a indicates that, while the GB moves, the riser is displaced along the glide plane of the $\boldsymbol{b}_{2/0}$ (red dotted line). Fig 5b shows in detail the displacement downwards of the riser due to the creation of $b_{2/2}$ that expand outwards and allow the boundary to migrate. If the stress is reversed the same mechanism operates (exchanging the sign of the $b_{2/2}$disconnections) and the GB is displaced upwards. Thus, the disconnection produced by the $\boldsymbol{b}_{2/0}$ facilitates the shear-coupled GB migration.

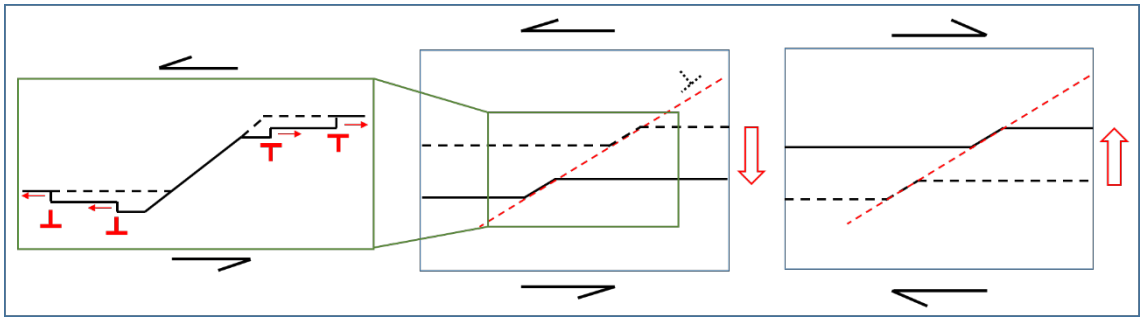

*Figure 5. Displacement of the GB with the $b_{8/6}$*disconnection*. The big red arrows indicate the direction of motion of the GB. Black arrows indicate the sense of shear stress. The red dotted line indicates the glide plane of the$b_{2/0}$dislocation; notice that the riser of the* disconnection *is displaced along this plane. (Green rectangle) Detail of the $b_{8/6}$ defect in the (3-32) GB acting as source of $b_{2/2}$ EDisc. A snapshot of $b_{8/6}$ is shown in fig.2a*

3.3.2 GB with a disconnection produced by the interaction with $\boldsymbol{b}_{-2/0}$ dislocation

The crystal dislocation $\boldsymbol{b}_{-2/0}$ under stress reacts with the GB forming the GBD $b_{-12/-10}$; its riser gradually orients along the $(1\bar{1}0)_\lambda$ plane. The interaction of this disconnection with the $\boldsymbol{b}_{2/2}$ EDisc differs from the interaction with the $\boldsymbol{b}_{-2/-2}$; as a consequence the displacement of the GB under shear stress depends on the sense of the shear, as shown schematically in figs. 6&7.

Under positive shear stress, $\boldsymbol{b}_{-2/-2}$ runs to the right (at 550MPa) and $\boldsymbol{b}_{2/2}$ runs to the left (at 620MPa). Therefore, $\boldsymbol{b}_{-2/-2}$ approaches the disconnection from its left side and

$\boldsymbol{b}_{2/2}$ approaches the disconnection from its right side. In both cases, there is no compensated climb.

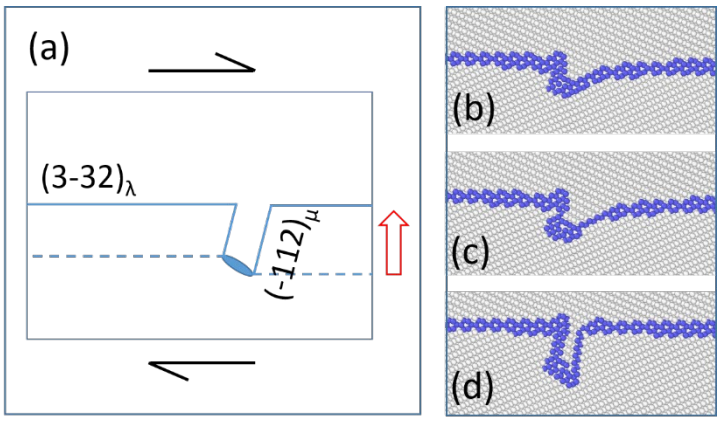

Figure 6. a) Displacement of the GB with the $b_{-12/-10}$ disconnection *and nucleation of the {112} twin. The red arrow indicates the direction of motion of the GB under the shear stress. Black arrows indicate the sense of shear stress. b-d) Snapshots showing the formation of the {112} twin from the GBD.*

The EDiscs $\boldsymbol{b}_{-2/-2}$ are stopped by the disconnection and pileup at its left side whereas $\boldsymbol{b}_{2/2}$ pileup at the right side forming a facet $\{112\}_\lambda/\{110\}_\mu$, as shown in fig 6b. When the facet is large enough it becomes unstable and transforms into a symmetric {112} facet forming the embryo of a {112} twin shown in fig. 6c.

When a negative shear stress is applied to the GB with a $b_{-12/-10}$ GBD, $\boldsymbol{b}_{2/2}$ EDiscs glide from the left side; when five of them pileup on the disconnection, the reaction (3) in section 3.2.1 is produced. Notice that the reaction is energetically feasible in both senses since the BVs form a right triangle (see fig. 1). The initial crystal dislocation is recovered and can glide along its own glide plane releasing stress, as shown in fig. 7; when relaxing to the new equilibrium, the reaction (3) is repeated and five EDiscs are emitted that continue gliding to the right. The same mechanism is found in the interaction of the (112) GB with a crystal dislocation, as presented in [21], although in that case only one disconnection is needed for the reaction to occur.

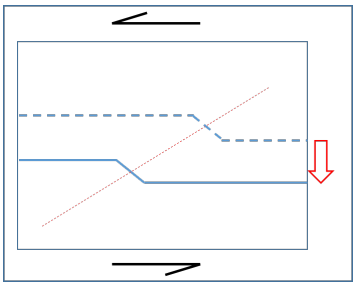

Figure 7. Displacement of the GB with the $b_{-12/-10}$disconnection *under a negative shear. The red dotted line indicates the glide plane of the incident*$b_{-2/0}$ *dislocation, notice that the riser of the* disconnection *is displaced along this plane. A snapshot of* $b_{-12/-10}$ *is shown in fig.2c*

3.3.3 GB with a GBD produced by the interaction with $\boldsymbol{b}_{\pm 4/0}$ dislocations (100°)

In the case of $\boldsymbol{b}_{4/0}$, the GBD is decomposed into two adjacent GBDs, i.e. $b_{12/10}$+$b_{-10/-12}$, with risers differently oriented, as shown in fig. 8a. This fact impedes that these risers

could move upwards and determines the behaviour of the GB under a positive shear stress.

Thus, under positive shear stress, the interaction of the EDisc with the GBD is as follows: $\boldsymbol{b}_{-2/-2}$ can interact with the GBD approaching from its left side and $\boldsymbol{b}_{2/2}$ can interact approaching the GBD from its right side (fig.8b). These EDisc move the GB upwards by two planes and return the GBD back to $\boldsymbol{b}_{2/-2}$. The following process of GB displacement is like for the disconnection $b_{-12/-10}$ described in section 3.3.2 and the same {112} twin embryo is formed as shown in fig. 8c&d, although the dislocation content at the tip of the twin is different in each case. The sustained growth of the twin is produced at a shear stress of 1.15 GPa.

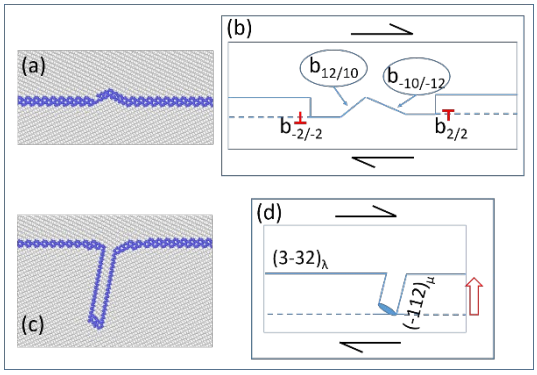

Figure 8. a) Core of the $b_{-2/2}$ GBD that relaxes into $b_{12/10}$ and $b_{-10/-12}$ disconnections. b) Under positive shear stress EDiscs approach the GBDs. c&d) {112} twin embryo created by successive glide of EDiscs

Under negative shear stress, initially a dipole of EDisc is created at the junction of the two facets and creates a plateau in between the facets, as shown in fig. 9. From then on, the mechanism presented in fig.5b operates in $b_{12/10}$ disconnection and the equivalent mechanism represented in the green rectangle of fig 9 operates on the $b_{-10/-12}$ disconnection. Both disconnections perform a compensated climb and move along their risers (dotted red line), as shown in fig. 9. The process is a conservative SCGBM. The steady state for the displacement downwards of the GB is produced at a stress of 1.35 GPa.

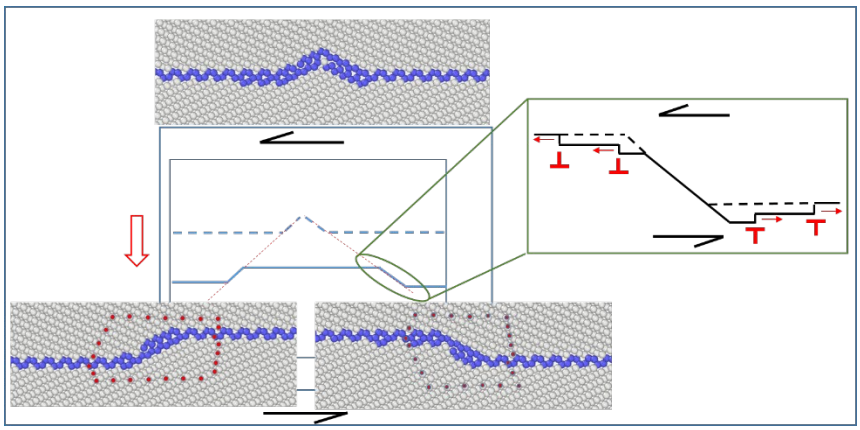

Figure 9. Displacement of the GB under a negative shear stress. The GB moves down and the disconnections $b_{12/10}$ *(left) and* $b_{-10/-12}$ *(right) moves with a compensated climb. The Burgers circuits used to analyse the two disconnections are marked in red. (Green rectangle) Detail of the mechanism of displacement of the riser of the* $b_{-10/-12}$disconnection.

In the case of $\boldsymbol{b}_{-4/0}$, the dislocation is attracted but not absorbed by the GB and it keeps its own BV. Under both, positive and negative shear stress, the dislocation is dragged by the GB while the GB is displaced upwards and downwards respectively.

3.3.4 GB with a GBD produced by the interaction with mixed $\boldsymbol{b}_{1/0}$ and $\boldsymbol{b}_{-1/0}$ dislocations

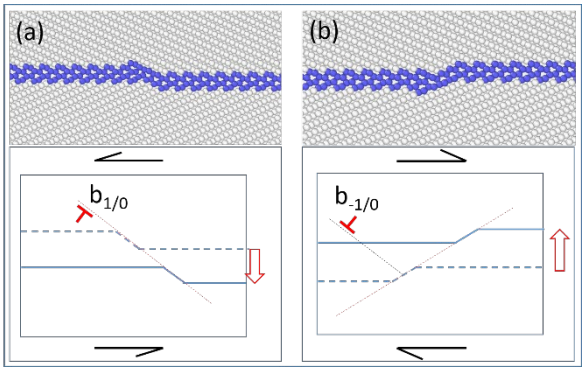

Figure 10. Displacement of the GB with the $\boldsymbol{b}_{-5/-6}$disconnection *(a) and* $\boldsymbol{b}_{3/4}$disconnection *(b). The initial crystal mixed dislocations (before reaction) with their glide planes are included.*

The screw part of the mixed dislocation is not modified by the reaction. Only the edge part transforms by emitting EDisc during the interaction. The resultant GBDs, $\boldsymbol{b}_{-5/-6}$ and $\boldsymbol{b}_{3/4}$, perform a compensated climb when the GB is displaced, as shown in fig. 10, and follow the GB with the mechanism described in section 3.3.1 and figs.5b and 9b. Thus, when the GB interacts with a mixed dislocation it performs a SCGBM.

3.4 Growth of the {112} twin

The {112} twin is initially nucleated either at the core of the $\boldsymbol{b}_{-12/-10}$ disconnection or the core of the $\boldsymbol{b}_{2/-2}$ GBD, when the GB is under a positive shear stress, i.e., the μ crystal, containing the twin, grows at expenses of the λ crystal (where the crystal dislocations come from).

The development of the twin is produced in several steps, as follows.

The gliding $\boldsymbol{b}_{\pm 2/\pm 2}$ EDisc cannot overcome these disconnections and pileup at both sides of the disconnection creating a twin embryo of four or six planes thick, depending on the core of the disconnection, as shown in figs. 6 and 8. The core of the disconnection forms the twin tip. In the first stage of growth, the twin, with a constant thickness, increases its length due to the displacement of the {332} GB but the twin tip is not moving.

The thickening of the twin starts when the EDisc associated to the twin boundary, i.e., $\boldsymbol{b}_{\pm 1/\pm 1}$ are produced [21]. This may occur at the pristine {112} boundary under a shear stress along the twin boundary of about 2.4 GPa, or at a smaller stress if there are stress concentrators [21].

The reaction of the intrinsic EDisc of the (112) twin boundary with the dislocation at the tip of the twin creates a glissile dislocation that run into the crystal. An example is shown in fig. 11, which corresponds to the reaction of the GB with the $\boldsymbol{b}_{4/0}$ crystal dislocation, increasing the length of the twin.

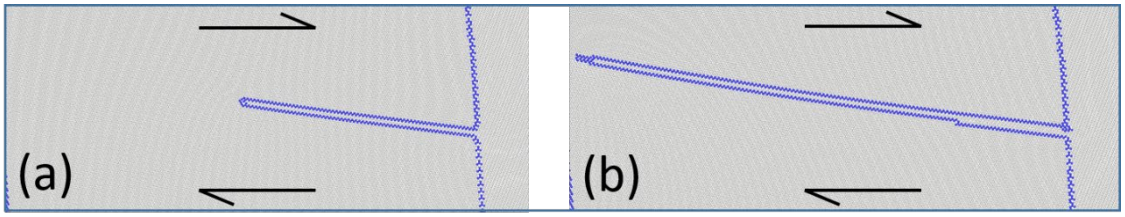

Figure 11. {112} twin under an applied shear stress (black arrows). a) The growth of the twin is produced by the motion of $(3\bar{3}2)$ *GB (vertical in the images). b) The twin thickens by glide of disconnection dipoles created at the twin boundary and increase its length by the transformation and glide of the tip.*

Let us describe the process in more detail. The misorientation of the {332} GB is 50.48˚ and the misorientation of the {112} GB is 70.53˚ (minimal possible misorientation angle is considered). Note that $\angle(1\bar{1}\bar{2})_\lambda/(1\bar{1}0)_\mu = 4.26°$ and $\angle(1\bar{1}2)_\lambda/(1\bar{1}\bar{2})_\mu = 20.04°$ for the {332} GB. The $\boldsymbol{b}_{2/2}$ disconnection has $(1\bar{1}\bar{2})_\lambda/(1\bar{1}0)_\mu$ facet in its core (Fig.1) and the pileup of such disconnections gliding on parallel $(3\bar{3}2)_\lambda$ planes produces the $(1\bar{1}\bar{2})_\lambda/(1\bar{1}0)_\mu$ facet shown in Fig.6. It is interesting that a row of $\boldsymbol{b}_{2/2}$ disconnections located along the bisection plane of $(1\bar{1}\bar{2})_\lambda$ and $(1\bar{1}0)_\mu$ (such plane is inclined to $(3\bar{3}2)_\lambda$ boundary by 27.4˚) is equivalent to a disclination dipole with Frank angle ω=4.26˚, i.e. this disclination dipole exactly compensates the misorientation between $(1\bar{1}\bar{2})_\lambda$ and $(1\bar{1}0)_\mu$ planes. However, the asymmetrical $(1\bar{1}\bar{2})_\lambda/(1\bar{1}0)_\mu$ facet becomes unstable, when it becomes longer. It transforms into the symmetrical $\{112\}$ twin boundary. Such transformation is possible because a row of $\boldsymbol{b}_{2/2}$ disconnections located

along bisect plane of $(1\bar{1}2)_\lambda$ and $(1\bar{1}\bar{2})_\mu$ planes is equivalent to disclination dipole with Frank angle ω=20.04˚. Such disclinations are settled in facet junctions and exactly compensate the misorientation between $(1\bar{1}2)_\lambda$ and $(1\bar{1}\bar{2})_\mu$ planes.

4. Discussion

The most significant intrinsic dislocations of the {332} <110> tilt GB are, on the one hand, the elementary disconnections, $\boldsymbol{b}_{\pm 2/\pm 2}$, responsible for the shear-coupled GB migration. The passage of each of them accommodates a shear due to its dislocation character and moves the GB by two planes due to its step. These disconnections may be produced in pairs at the pristine GB or at centres of stress concentration. On the other hand, there are the GB dislocations produced by the interaction of the GB with the crystal dislocations, $\frac{1}{2}\langle 111\rangle$. Their reaction with the GB depends on the orientation and sense of the Burgers vector. Therefore, considering all possible orientations of $\frac{1}{2}\langle 111\rangle$, there are six different reactions producing six GBD's that, in turn, may act as sources of $\boldsymbol{b}_{\pm 2/\pm 2}$. The final product of each reaction is a GBD (with or without step) and several glissile disconnections that glide away. The BV of the GBD is, in general, not parallel to the GB; therefore, the GBD cannot glide along the GB.

A GB in a polycrystal submitted to an external shear stress may have several GBDs that will interact with the gliding $\boldsymbol{b}_{\pm 2/\pm 2}$. Since the sense of the applied shear stress may result in a different reaction between the elementary disconnections and the GBD, we should consider twelve cases. These reactions are reduced to two possible scenarios when viewed at a higher scale: a) In general, with only two exceptions, the two interacting GB defects may climb over each other in a compensated climb and the GBD moves together with the GB in a conservative manner (no atomic diffusion is needed) producing shear-coupled GB migration. b) The two exceptions occur for a positive shear stress when the μ crystal grows at the expenses of the λ crystal (where the crystal dislocations come from). Then, the core of the GBD does not allow a compensated climb. The accumulation of $\boldsymbol{b}_{\pm 2/\pm 2}$ at each side of the GBD nucleates a (112) twin embryo. In this case, the displacement of the GB is produced by the glide of disconnections that pileup forming the boundaries of the twin. In a second stage, the twin boundary creates disconnection dipoles that thicken the twin and react with the tip that emits dislocations, increasing the length of the twin.

In both scenarios, the motion of the GB due to the glide of disconnections, with or without creation of a twin, accommodates the plastic deformation.

5. Summary and Conclusions

The interaction of a single crystal dislocation, ½ <111>, with the [110]($3\bar{3}2$) tilt grain boundary in bcc Fe has been studied at the atomic level using MD simulations. All the orientations and senses of the crystal dislocation have been considered.

The GB has absorbed the dislocations, either due to its mutual attraction or under an applied shear stress. The reaction and final defects at the GB depend on the orientation of the glide plane, the sign of the Burgers vector and the edge or mixed character of the dislocation.

Dislocation with Burgers vector inclined 29.5º to the GB: When the dislocation has a Burgers vector that forms an acute angle with the GB ($b_{2/0}$), it transforms into several elementary disconnections that glide away and a GBD with core along the glide plane of the crystal dislocation; the core forms a facet $\{112\}_\lambda/\{110\}_\mu$.When a shear stress is applied, the GBD acts as a source of elementary disconnection dipoles ($\boldsymbol{b}_{2/2}$) that glide along the GB allowing its displacement. Thus, the GBD facilitates the shear-coupled GB migration.

If the Burgers vector forms an obtuse angle with the GB ($b_{-2/0}$), the core of the GBD forms an angle of 126º to the glide plane of the dislocation and forms a facet $\{110\}_\lambda/\{112\}_\mu$. The number of elementary disconnections emitted depends on the temperature and local stresses. Under a *positive* shear stress, elementary disconnections of opposite sign, gliding along the GB, are stopped by the GBD. They pileup at the left and right side of the GBD respectively, forming a facet $\{112\}_\lambda/\{110\}_\mu$. When the facet is large enough it becomes unstable and transforms into a symmetric {112} facet forming the embryo of a {112} twin. Under a *negative* shear stress, the sign of disconnections is reversed and the shear-coupled GB migration operates.

Dislocation with Burgers vector inclined 100º to the GB: ($b_{4/0}$) there is attraction and absorption by the GB. The GBD created ($b_{2/-2}$) does not step the GB but, under relaxation, its core is decomposed into two GBDs, each of them with a facet (see fig. 8 for details). This fact impedes that these risers could move upwards and determines the behaviour of the GB under a *positive* shear stress, i.e., a (112) twin embryo is created. Under *negative* shear stress the risers can move down independently and the shear-coupled GB migration operates.

Changing the sign of the dislocation ($b_{-4/0}$), there is repulsion between the dislocation and the GB. The dislocation overcomes the repulsion if a shear stress of 1.3GPa is applied. Then, the dislocation stays attached to the GB but it keeps its Burgers vector. When the GB is displaced, under shear stress, by the passage of disconnections, it drags the dislocation.

Dislocation with mixed Burgers vector gliding along the $(1\bar{1}0)$: A GBD is created, which screw part is unchanged and the edge part has a core forming a facet $(1\bar{1}0)_\lambda/(1\bar{1}2)_\mu$. The reaction creates three elementary disconnections that run away. Changing sign changes the orientation of the riser that is inclined to the glide plane with a facet $(1\bar{1}2)_\lambda/(1\bar{1}0)_\mu$. Under shear stress for both signs of Burgers vector and stress the GB performs a shear-coupled migration.

Thus, to conclude, the (332) tilt GB performs a shear coupled migration when the elementary disconnections can climb conservatively along the GBD; otherwise, a twin

embryo is created at the place of the GBD. This GB accommodates deformation by combining the shear-coupled GB migration and the formation of (112) twins

Acknowledgments

This work was supported by the Euratom research and training programme 2014-2018 under grant agreement No 755039 (Project M4F), by the Spanish MINECO: FIS2015-69017-P. This work also contributes to the Joint Program on Nuclear Materials (JPNM) of the European Energy Research Alliance (EERA).

Data availability

All the information required to reproduce these findings is included in the Methodology Section.

References

1. A. P. Sutton, R.W. Balluffi, Interfaces in crystalline materials (Chapter 12), Oxford classic series, 2006
2. J. Liu, C. Chen, Q. Feng, X. Fang, H. Wang, F. Liu, J. Lu, D. Raabe, Mater Sci&Eng A, 703 (2017) 236
3. W.Z. Abuzaid, M.D. Sangid, J.D. Carroll, H. Sehitoglu, J. Lambros, J. Mech. Phys. Solids 60 (2012) 1201
4. A. Rajabzadeh, F. Mompiou, S. Lartigue-Korinek, N.Combe, M.Legros, D.A.Molodov, Acta Mater., 77 (2014) 223
5. K. D. Molodov, T. Al-Samman, D. A. Molodov, S. Korte-Kerzel,Acta Mater., 134 (2017) 267
6. D.E. Spearot, K.I. Jacob and D.L. McDowell, Acta Mater., 53 (2005) 3579-3589
7. A. Serra, D.J. Bacon, Mater. Sci. Eng. A 400–401 (2005) 496
8. J. Wang, J.P. Hirth, C.N. Tomé,Acta Mater., 57 (2009) 5521
9. F. Wang, C.D. Barrett, R.J. McCabe, H. El Kadiri, L. Capolungo, S.R. Agnew, Acta Mater, 165 (2019) 471
10. R.C. Pond, Line defects in interfaces, in: Dislocations in Solids, Edited by F.N.R. Nabarro. Amsterdam: North Holland, 1989, Vol. 8, p.1
11. J.P. Hirth, J. Phys. Chem. Sol., 1994, 55, 985
12. A.Ostapovets, A.Serra, Metals, 10 (2020) 1134
13. H.A. Khater, A. Serra, R.C. Pond, J. P. Hirth, Acta Mater.,60 (2012) 2007
14. H.A. Khater, A. Serra, R.C. Pond,, Philos Mag, 93 (2013) 1279
15. R. C. Pond, J. P. Hirth, A. Serra and D. J. Bacon, Materials Research Letters, 4 (2016) 185
16. A.Serra, N.Kvashin, N.Anento, Letters on Materials, 10 (2020) 537

17. R. C. Pond, J. P. Hirth, H.A. Khater, A. Serra, Mater. Sci. Forum, 753(2013) 125
18. N.Anento, A. Serra, Comp. Mater. Sci. 179(2020) 109679
19. R. C. Pond, A. Serra, and D. J. Bacon, Acta Mater. 47 (1999) 1441.
20. A. Serra, D.J. Bacon, Philos. Mag. A 73 (1996) 333.
21. N. Kvashin, P. L. García-Müller , N. Anento, A. Serra, Phys. Rev. Mater., 4 (2020) 073604
22. A. Ostapovets, A. Serra Philos. Mag., 94 (2014) 2827
23. J.E. Brandenburg, M. Schoof, D. A. Molodov, Philos. Mag. Letters, 100 (2020) 10
24. F. Mompiou, M. Legros, D. Caillard, J Mater Sci, 46 (2011) 4308
25. A. Rajabzadeh, M. Legros, N. Combe, F. Mompiou, D.A. Molodov, Philos. Mag, 93 (2014) 10
26. Q. Zhu, S.C. Zhao, C. Deng, X.H. An, K.X. Song, S.X. Mao, J.W. Wang, Acta Mater. 199 (2020) 42
27. N. Combe, F. Mompiou, and M. Legros, Phys. Rev. Materials 3, (2020) 060601
28. M. Dupraz, S.I. Rao, H. Van Swygenhoven, Acta Mater 174 (2019) 16-28
29. D. Chen, S. Xu, Y. Kulkarni, Phys. Rev. Mater 4 (2020) 033602
30. I.J. Beyerlein, X. Zhang, A. Misra, Annu Rev. Mater. Res. 44 (2014) 329
31. C. Wei, L. Zhang, J. Han, D. J. Srolovitz, Y. Xiang, SIAM Journal on Applied Mathematics. 80 (2020) 1101-1122
32. S. L. Thomas, C. Wei, J. Han, Y. Xiang, D. J. Srolovitz, PNAS 116 (2019) 8756
33. N. Kvashin, N. Anento, D. Terentyev, A. Bakaev, A. Serra, Phys Rev Mater. (2021) DOI: 10.1103/PhysRevMaterials.5.013605
34. A.A. Popov, A.V. Litvinov, A.G. Illarionov, The Physics of Metals & Metallography, 89 (2000) 1
35. G. M. Rusakov, A. V. Litvinov, V. S. Litvinov, Metal Sci. & Heat Treatment, 48 (2006) 244
36. I. Gutierrez-Urrutia, C.L. Li, S. Emura, X. Min, K. Tsuchiya, Sci. & Tech. Advanced Mater., 17 (2016) 220
37. S. Plimpton, J Comp Phys, 117, (1995) 1
38. G. Ackland, M.I.Mendelev, D.J.Srolovitz, S. Han, A.V. Barashev, J. Phys. Condens. Matter 16, (2004) S2629
39. D. Terentyev, X. He, A. Serra, and J. Kuriplach, Comput. Mater. Sci. 49(2010) 419
40. P. Hirel, Comput. Phys. Comm. 197 (2015) 212
41. A. Stukowski Modelling Simul. Mater. Sci. Eng. 18 (2010) 015012
42. T. Braisaz, P. Ruterana, G. Nouet, A. Serra, Th. Karakostas, T. Kehagias, Philos. Mag. Letters, 74 (1996) 331